

## MAJOR PAPER

# Evaluation of Red Degeneration of Uterine Leiomyoma with Susceptibility-weighted MR Imaging

Mayumi Takeuchi<sup>1\*</sup>, Kenji Matsuzaki<sup>2</sup>, Yoshimi Bando<sup>3</sup>, and Masafumi Harada<sup>1</sup>

**Purpose:** Red degeneration of uterine leiomyoma (RDL) is a hemorrhagic infarction caused by peripheral venous thrombosis. The peripheral high-intensity rim on  $T_1$ -weighted MRI is characteristic for RDL; however, it may not be observed at all the phases of RDL. Susceptibility-weighted MR sequences (SWS) have exquisite sensitivity to blood products, and we hypothesized that the low-intensity rim due to the  $T_2^*$  shortening effects of blood products may be more clearly demonstrated on SWS. The purpose of this study is to evaluate the capability of SWS for the diagnosis of RDL.

**Methods:** Surgically proven 15 RDL, which showed suggestive MRI findings (high-intensity rim or entirely high signal intensity on  $T_1$ -weighted imaging) were retrospectively evaluated. MRI was qualitatively evaluated for the presence of high-intensity rim around a mass on fat-saturated  $T_1$ -weighted images, and low-intensity rim on  $T_2$ -weighted images and on SWS (susceptibility-weighted imaging [SWI] or  $T_2$ -star-weighted angiography [SWAN]).

**Results:** The high-intensity rim on  $T_1$ -weighted images, low-intensity rim on  $T_2$ -weighted images and on SWS were observed in 47%, 47%, and 100% of RDL, respectively. The other 53% of lesions showed entirely high signal intensity on  $T_1$ -weighted images. Pathological examination revealed coagulative necrosis in all 15 lesions.

**Conclusion:** SWS may be helpful for the diagnosis of RDL by revealing characteristic peripheral low-intensity rim.

**Keywords:** leiomyoma, red degeneration, susceptibility-weighted magnetic resonance sequence, uterus, uterine sarcoma

## Introduction

Red degeneration of uterine leiomyoma (RDL) is a subtype of degeneration, which often occurs during pregnancy, or with the use of oral contraceptives.<sup>1,2</sup> On gross pathological examination, it is characterized by a red, hemorrhagic appearance of the leiomyoma if the surgery was performed during the acute phase of red degeneration. Red degeneration is a massive hemorrhagic infarction of leiomyoma caused by venous thrombosis within the periphery of a leiomyoma. Characteristic signal intensity patterns have been described on MRI as a peripheral high-intensity rim on  $T_1$ -weighted images due to

the  $T_1$  shortening effects of methemoglobin of blood products confined to the thrombosed numerous dilated vessels surrounding the tumor.<sup>1-4</sup> On  $T_2$ -weighted images, it may show variable signal intensity with a low-intensity rim due to the  $T_2^*$  shortening effects of deoxyhemoglobin, intracellular methemoglobin, or hemosiderin of blood products also confined to the thrombosed vessels.<sup>1-4</sup> However, the high-intensity rim on  $T_1$ -weighted images may not be observed at the very acute phase of red degeneration because of insufficient conversion of deoxyhemoglobin into methemoglobin, the low-intensity rim on  $T_2$ -weighted images due to deoxyhemoglobin may be observed even at the very acute phase. However, because usual leiomyomas show low signal intensity on  $T_2$ -weighted images, a peripheral rim-like low-intensity due to the residual un-degenerated area could be observed in degenerated leiomyoma without hemorrhagic infarction.

Susceptibility-weighted MR sequences (SWS) such as susceptibility-weighted imaging (SWI) and  $T_2$ -star-weighted angiography (SWAN) can maximize sensitivity to susceptibility effects, and have exquisite sensitivity to blood products.<sup>5-8</sup> We hypothesized that the low-intensity rim due to the  $T_2^*$  shortening effects of blood products may be more

<sup>1</sup>Department of Radiology, Tokushima University, 3-18-15 Kuramoto-cho, Tokushima, Tokushima 770-8503, Japan

<sup>2</sup>Department of Radiological Technology, Tokushima Bunri University, Tokushima, Japan

<sup>3</sup>Division of Pathology, Tokushima University Hospital, Tokushima, Japan

\*Corresponding author, Phone: +81-88-633-9283, Fax: +81-88-633-7468, E-mail: mayumi@tokushima-u.ac.jp

©2018 Japanese Society for Magnetic Resonance in Medicine

This work is licensed under a Creative Commons Attribution-NonCommercial-NoDerivatives International License.

Received: May 9, 2018 | Accepted: July 11, 2018

clearly demonstrated on SWS and be helpful for the diagnosis of red degeneration. The purpose of this study was to evaluate the capability of SWS for the diagnosis of red degeneration of uterine leiomyomas.

## Materials and Methods

### Patients

The Institutional Review Board in our hospital approved this retrospective study, and waived the requirement for written informed consent of patients. We cross-referenced the database of the Department of Obstetrics and Gynecology to identify all patients with histologically proven leiomyomas with possible red degeneration who had undergone MRI examinations including SWS between May 2010 and April 2016. Lesions with suggestive MRI findings for red degeneration such as well demarcated uterine myometrial masses exhibiting high-intensity rim or entirely high signal intensity compared to the uterine myometrium on T<sub>1</sub>-weighted imaging were included in this study. The patients were with or without suggestive symptoms for red degeneration (lower abdominal pain and/or fever) and suspected risk factors for onset (pregnancy, use of oral contraceptives, or hormonal drug administration such as gonadotropin-releasing hormone antagonist). All lesions were re-reviewed by a pathologist with 19 years of experience in gynecological pathology. A total of 15 lesions in nine women with a mean age of 39 years (range, 27–52 years) were included in the current study (Table 1). The median time from MRI examination to operation was 91 days (range 12–188). The risk factors for onset were pregnancy for five patients and

hormonal drug administration for one patient; however, the other three patients did not have any risk factors. The median lesion size, which was the longest diameter measured by MRI was 59 mm (range, 18–88 mm).

### Magnetic resonance imaging

Thirteen leiomyomas with red degeneration in seven patients were evaluated at 1.5T (Signa Excite HD or HDx, General Electric, Milwaukee, WI, USA), whereas two leiomyomas with red degeneration in two patients were evaluated at 3T (Signa 3T HD or Discovery MR750, General Electric) by using body-array torso coils. SWI consisting of both magnitude and phase images from 2D fast spoiled gradient recalled acquisition in the steady-state sequence (TR/TE, 650–700/30 ms; flip angle, 15–20 degrees; matrix size, 288 × 192; FOV, 28 × 28 cm; two signals acquired; section thickness, 8 mm; section gap, 1 mm) were obtained in two leiomyomas with red degeneration. Sequence parameters in 3T and 1.5T were almost identical except for flip angles (15 degrees in 3T, and 20 degrees in 1.5T). SWAN using multiple magnitude images with different echo times for the image generation: 3D multi-echo gradient echo (TR/TE, 42.9/27.5 ms for 3T and 78.8/49 ms for 1.5T; matrix size, 320 × 192–256; FOV, 28 × 28 cm; section thickness, 3–5 mm; spacing, 1.5–2.5 mm) were obtained in 13 leiomyomas with red degeneration. Fast spin-echo T<sub>2</sub>-weighted images (TR/TE, 4000–7000/99.3–100 ms) and spin-echo (TR/TE, 466.7–600/7.9–9.8 ms) or fast spoiled gradient-recalled echo (TR/TE, 2.9–4/1.3–1.7 ms) T<sub>1</sub>-weighted images with fat saturation were obtained in all patients.

**Table 1** Clinical courses, MRI findings, and pathological findings of patients

Case	Age	Lesion	Risk factor	Symptom	Size	MRI findings			Pathological findings			
						T <sub>1</sub> -high	T <sub>2</sub> -low	SWS-low	C.N.	H.D.	Hem.	V.T.
1	27	1	None	Pain	60	rim	rim	rim / s-m	+	+	+	
2	45	2	None	Pain	75	rim	rim	rim / s-m	+		+	
3	32	3	Pregnancy	Pain	118	rim	rim	rim	+	+		
4	52	4	None	Pain	99	rim	rim	rim	+	+		
5	42	5	Drug*	Anemia	56	rim	rim	rim / s-m	+	+		
6	35	6	Pregnancy	Pain	50	diffuse	diffuse	rim / s-m	+	+	+	
		7			18	diffuse	diffuse	rim / s-m	+	+	+	
		8			25	diffuse	diffuse	rim / s-m	+	+	+	
		9			29	diffuse	diffuse	rim / s-m	+	+	+	
		10			51	diffuse	diffuse	rim / s-m	+	+	+	
		11			27	diffuse	diffuse	rim / s-m	+	+	+	
		12			76	diffuse	diffuse	rim / s-m	+	+	+	
7	35	13	Pregnancy	None	66	diffuse	rim	rim / s-m	+	+	+	probable
8	40	14	Pregnancy	None	49	rim	diffuse	rim / s-m	+	+		
9	39	15	Pregnancy	Pain	84	rim	rim	rim / s-m	+	+	+	

\*Drug, Gonadotropin-releasing hormone antagonist; s-m, spotty to mottled signal voids; C.N., coagulative necrosis; H.D., hyalinized degeneration; Hem., hemosiderin deposits; V.T., venous thrombus. SWS, Susceptibility-weighted MR sequences.

### Analysis methods

Two radiologists with 27 and 18 years of experiences in gynecological MRI qualitatively evaluated the images for the presence of a low-intensity rim around a mass on T<sub>2</sub>-weighted images and on SWS, and of a high-intensity rim around a mass on fat-saturated T<sub>1</sub>-weighted images. Both iso intensity mass compared to the myometrium with high-intensity rim and high-intensity mass compared to the myometrium with higher intensity rim were considered as “high-intensity rim” on fat-saturated T<sub>1</sub>-weighted images. The reviewers examined all MR images of the cases independently, and then resolved discrepancies by consensus.

### Results

The high-intensity rim on T<sub>1</sub>-weighted images was observed in seven of 15 leiomyomas with red degeneration (47%) (Fig. 1), whereas the other eight leiomyomas with red degeneration (53%) showed entirely high signal intensity and the high-intensity rim was not clearly demonstrated (Fig. 2). The low-intensity rim on T<sub>2</sub>-weighted images was observed in seven of 15 leiomyomas with red degeneration (47%) (Fig. 1). The low-intensity rim on SWS was observed in all 15 leiomyomas with red degeneration (100%) (Figs. 1 and 2). Spotty or mottled signal voids within the tumors were observed in 13 of 15 leiomyomas with red degeneration (87%) (Fig. 1).

Pathological examination of the leiomyomas with red degeneration revealed coagulative necrosis in all 15 lesions, hyaline degeneration in 14 lesions, and obsolete hemorrhage (hemosiderin deposition) in 11 lesions. Probable peripheral venous thrombus was found in only one lesion.

### Discussion

In the current study, the low-intensity rim on SWS was observed in all the leiomyomas with red degeneration,

whereas the high-intensity rim on fat-saturated T<sub>1</sub>-weighted images was observed in 47% of the leiomyomas with red degeneration. According to the results, both SWS and fat-saturated T<sub>1</sub>-weighted images can provide specific information for the diagnosis of leiomyoma with red degeneration. SWS may be more sensitive for the presence of blood products than fat-saturated T<sub>1</sub>-weighted images.

Leiomyomas are the most common benign uterine neoplasm, which is composed of smooth muscle and varying amounts of fibrous tissue with/without various types of degeneration, such as hyaline, hydropic, myxoid, cystic, fatty, or red degeneration.<sup>2</sup> Red degeneration (carneous degeneration) is a hemorrhagic infarction of uterine leiomyoma, which may cause acute abdominal pain. Because leiomyomas with red degeneration can be treated conservatively, preoperative diagnosis is important.<sup>1</sup> Leiomyomas with red degeneration may show diffuse high signal intensity or a peripheral high-intensity rim on T<sub>1</sub>-weighted images depending on the degree of intra-tumoral hemorrhage, coagulative necrosis, or hyaline degeneration.<sup>1-4</sup> The peripheral high-intensity rim on T<sub>1</sub>-weighted images reflecting methemoglobin of blood products confined to the thrombosed vessels is characteristic; however, this finding may not be observed at the very acute phase of red degeneration. Because oxyhemoglobin and deoxyhemoglobin do not cause the signal increase on T<sub>1</sub>-weighted images, high signal intensity due to the T<sub>1</sub> shortening effect of methemoglobin may be observed at least 3 days after the onset.<sup>9,10</sup> The peripheral low-intensity rim on T<sub>2</sub>-weighted images due to the T<sub>2</sub><sup>\*</sup> shortening effect of deoxyhemoglobin, intracellular methemoglobin or hemosiderin reflecting venous thrombosis is also characteristic for red degeneration, and may be observed even at the very acute phase due to deoxyhemoglobin. However, usual leiomyoma itself may show low signal intensity on T<sub>2</sub>-weighted images and evaluation of the low-intensity rim may occasionally be difficult. In our study, the prevalence of the high-intensity rim

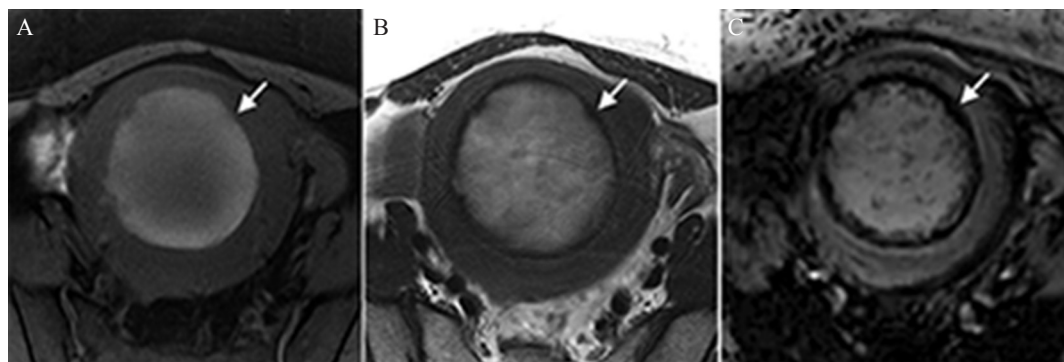


**Fig. 1** A 45-year-old woman with uterine leiomyoma with red degeneration. (A) On the fat-saturated T<sub>1</sub>-weighted image, a peripheral high-intensity rim (arrow) is clearly demonstrated surrounding a uterine myometrial mass exhibiting iso to slight high signal intensity compared with the myometrium. (B) The mass shows high signal intensity with a low-intensity rim (arrow) on T<sub>2</sub>-weighted image. (C) A low-intensity rim (arrow) on susceptibility-weighted imaging (SWI) is more prominent than that on T<sub>2</sub>-weighted image. Spotty low intensities are also observed within the mass on SWI.

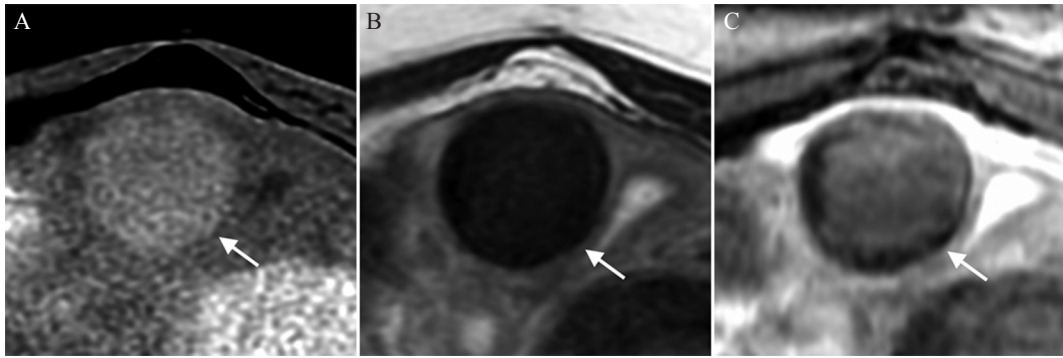


**Fig. 2** A 35-year-old woman with uterine leiomyomas with red degeneration. (A) On fat-saturated  $T_1$ -weighted image, one of a uterine myometrial masses (arrow) shows diffuse high signal intensity compared with the myometrium and no peripheral high-intensity rim is demonstrated. (B) The mass shows diffuse low signal intensity (arrow) and no peripheral low-intensity rim is demonstrated on  $T_2$ -weighted image. (C) A low-intensity rim (arrow) is demonstrated on  $T_2$ -star-weighted angiography (SWAN).

on  $T_1$ -weighted images was only 47% (7 of 15 lesions), and the other eight lesions showed entirely high signal intensity compared to the myometrium. Nakai et al. evaluated the MRI and pathological findings of 10 leiomyomas with red degeneration, and the high-intensity rim on  $T_1$ -weighted images was found in only four lesions (40%). The other six lesions showed entirely high-intensity on  $T_1$ -weighted images and pathological examination revealed that coagulative necrosis without hemorrhage may cause high signal intensity of the lesions, and our results support their observation.<sup>4</sup>

Intra-tumoral necrosis and hemorrhage are suggestive findings for high-grade uterine sarcomas.<sup>11</sup> Because uterine sarcomas such as leiomyosarcoma could also show diffuse high signal intensity due to massive hemorrhagic necrosis, diagnosis of tumors exhibiting diffuse high signal intensity on  $T_1$ -weighted images may be problematic.<sup>11</sup> The low-intensity rim on  $T_2$ -weighted images was found in 7 of 15 leiomyomas with red degeneration (47%) exhibiting diffuse high signal intensity in our study, and the other eight lesions showed entirely or inhomogeneously low signal intensity so the presence of low-intensity rim was obscure on  $T_2$ -weighted images.

SWS such as SWI and SWAN are sensitive MRI techniques for blood products, and could demonstrate hemorrhage of various time phases.<sup>5–8</sup> SWS may reveal venous thrombus as signal voids due to the  $T_2^*$  shortening effects of both deoxyhemoglobin and intracellular methemoglobin at the acute phase and hemosiderin at the chronic to obsolete phases of thrombus.<sup>12</sup> In the current study, SWS demonstrated the peripheral low-intensity rim in all cases of leiomyomas with red degeneration. However, probable peripheral venous thrombus was pathologically revealed only in one lesion of leiomyomas with red degeneration, SWS could reveal hemosiderin deposits as remaining traces of obsolete venous thrombus in the other lesions. From the result, SWS may be helpful in distinguishing leiomyomas

with red degeneration from usual leiomyomas with degeneration or uterine sarcomas with massive hemorrhagic necrosis by revealing the peripheral low-intensity rim.

The retrospective nature and small population are limitations in this study. Use of multiple field strength and multiple SWS may be another limitations. Further studies in larger populations to verify the results are needed.

## Conclusion

We conclude that SWS may be helpful for the diagnosis of leiomyomas with red degeneration by revealing characteristic peripheral low-intensity rim.

## Conflicts of Interest

The authors declare that they have no conflicts of interest.

## References

1. Kawakami S, Togashi K, Konishi I, et al. Red degeneration of uterine leiomyoma: MR appearance. *J Comput Assist Tomogr* 1994; 18:925–928.
2. Murase E, Siegelman ES, Outwater EK, Perez-Jaffe LA, Tureck RW. Uterine leiomyomas: histopathologic features, MR imaging findings, differential diagnosis, and treatment. *Radiographics* 1999; 19:1179–1197.
3. Roche O, Chavan N, Aquilina J, Rockall A. Radiological appearances of gynaecological emergencies. *Insights Imaging* 2012; 3:265–275.
4. Nakai G, Yamada T, Hamada T, et al. Pathological findings of uterine tumors preoperatively diagnosed as red degeneration of leiomyoma by MRI. *Abdom Radiol (NY)* 2017; 42: 1825–1831.
5. Haacke EM, Xu Y, Cheng YC, Reichenbach JR. Susceptibility weighted imaging (SWI). *Magn Reson Med* 2004; 52: 612–618.
6. Boeckh-Behrens T, Lutz J, Lummel N, et al. Susceptibility-weighted angiography (SWAN) of cerebral veins and

- arteries compared to TOF-MRA. *Eur J Radiol* 2012; 81: 1238–1245.
7. Sehgal V, Delproposto Z, Haddar D, et al. Susceptibility-weighted imaging to visualize blood products and improve tumor contrast in the study of brain masses. *J Magn Reson Imaging* 2006; 24:41–51.
  8. Löbel U, Sedlacik J, Sabin ND, et al. Three-dimensional susceptibility-weighted imaging and two-dimensional T2\*-weighted gradient-echo imaging of intratumoral hemorrhages in pediatric diffuse intrinsic pontine glioma. *Neuroradiology* 2010; 52:1167–1177.
  9. Dooms GC, Uske A, Brant-Zawadzki M, et al. Spin-echo MR imaging of intracranial haemorrhage. *Neuroradiology* 1986; 28:132–138.
  10. Bradley WG Jr. MR appearance of hemorrhage in the brain. *Radiology* 1993; 189:15–26.
  11. Sahdev A, Sohaib SA, Jacobs I, Shepherd JH, Oram DH, Reznek RH. MR imaging of uterine sarcomas. *AJR Am J Roentgenol* 2001; 177:1307–1311.
  12. Takeuchi M, Matsuzaki K, Harada M. Susceptibility-weighted imaging of ovarian torsion: a case report. *Magn Reson Med Sci* 2015; 14:355–358.